



HAL
open science

Dissociation mechanisms of dissolved alkali silicates in sodium hydroxide

Romain Dupuis, Roland J.-M. Pellenq, Jean-Baptiste Champenois, Arnaud Poulesquen

► **To cite this version:**

Romain Dupuis, Roland J.-M. Pellenq, Jean-Baptiste Champenois, Arnaud Poulesquen. Dissociation mechanisms of dissolved alkali silicates in sodium hydroxide. *Journal of Physical Chemistry C*, 2020, 124 (15), pp.8288-8294. 10.1021/acs.jpcc.0c01495 . cea-03331870

HAL Id: cea-03331870

<https://cea.hal.science/cea-03331870v1>

Submitted on 5 Dec 2024

HAL is a multi-disciplinary open access archive for the deposit and dissemination of scientific research documents, whether they are published or not. The documents may come from teaching and research institutions in France or abroad, or from public or private research centers.

L'archive ouverte pluridisciplinaire **HAL**, est destinée au dépôt et à la diffusion de documents scientifiques de niveau recherche, publiés ou non, émanant des établissements d'enseignement et de recherche français ou étrangers, des laboratoires publics ou privés.



Distributed under a Creative Commons Attribution 4.0 International License

Dissociation Mechanisms of Dissolved Alkali Silicates in Sodium Hydroxide

Romain Dupuis,* Roland Pellenq, Jean-Baptiste Champenois, and Arnaud Poulesquen

Cite This: *J. Phys. Chem. C* 2020, 124, 8288–8294

Read Online

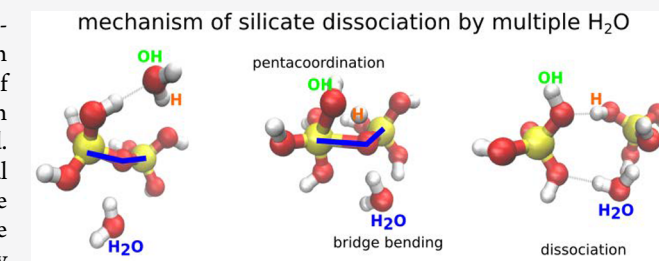
ACCESS |

Metrics & More

Article Recommendations

Supporting Information

ABSTRACT: Recent accelerated simulations of the decondensation of silicates by sodium hydroxide open a window on understanding complex mechanisms of the depolymerization of silicate chains. Herein, complex mechanisms of decondensation that involve two water molecules (or OH⁻ groups) are unveiled. The study of two different solutions, having the same chemical composition but in different concentration, help one to draw more general conclusions on the dissociation mechanism in silicate solutions. We find that the dissociation is not always assisted by single water molecules but that in about 20% of the cases two water molecules (or OH⁻) are present in the near environment. The results underline the importance to consider explicit water solvent in which water molecules are reactive.



I. INTRODUCTION

For a long time, efforts have been done to investigate and control the silicate chemistry.^{1–9} It is the base for the formation or phase transformation of liquids, gels, and minerals, yet it is unclear how water and silicate chains interplay at the atomic scale, depending on the chemistry of the solution and on the shape of the interface.^{10,11} It is mainly due to the complexity with experimentally characterizing the structure of silicates in solution.¹² Besides, molecular dynamics have helped to rationalize the outcomes of experiments. Until recently, it was also challenging to reproduce the bond formation or dissociation by atomistic simulations due to the high activation energy barrier (a few tenths of an electronvolt) to make or break Si–O bonds,^{13–15} but new methods have been used to produce reliable silicate structures.^{14,16,17} This opens the paths to study in detail the statistics of the mechanisms of decondensation for silicate chains. Indeed, long-time trajectories offer a large set of configurations of interest to observe multiple bond-breaking incidents.

In this work, we employ statistical analysis to describe the dissociation mechanisms, triggered by the addition of sodium hydroxide, that has been reproduced by accelerated molecular dynamics. The loss of connectivity is compared to experiments for two different solutions. Both systems contain sodium silicates in solution. In particular, we detail how several water molecules or OH⁻ groups could participate in bond dissociation.

II. METHODS

II.A. Experimental Samples. The chemical composition of the two sodium silicate solutions were adjusted according to

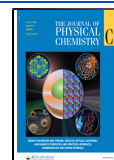
the final products we wanted to synthesize. The first one (named Zsol) is usually used to synthesize some aluminosilicate zeolites. The initial concentrations are [Si] = 2.25 mol·L⁻¹ and [Na⁺] = 1.31 mol·L⁻¹, which correspond to molar ratios of SiO₂/Na₂O = 2.44 and H₂O/Na₂O = 85. A sodium hydroxide solution ([NaOH] = 1.31 mol·L⁻¹) is added to this solution in order to study the silicate decondensation process, as explained by Dupuis et al. in 2019.¹⁷ The final concentrations are [Si] = 1.125 mol·L⁻¹ and [Na⁺] = 1.31 mol·L⁻¹ (final molar ratios are SiO₂/Na₂O = 1.72 and H₂O/Na₂O = 85). The second one (named Gsol) is commonly used to synthesize alkali-activated materials as geopolymers. Two solutions were characterized by varying the concentration of sodium hydroxide at fixed silicate and water content ([Si] = 5.8 mol·L⁻¹ and [Na⁺] = 9.66 mol·L⁻¹, which correspond to molar ratios of SiO₂/Na₂O = 1.2 and H₂O/Na₂O = 11.5, and [Si] = 5.8 mol·L⁻¹ and [Na⁺] = 13 mol·L⁻¹, which correspond to molar ratios of SiO₂/Na₂O = 0.89 and H₂O/Na₂O = 11.5).⁹

The NMR spectra corresponding to the two solutions are presented in Figure 1 in the initial state and after decondensation. As usually observed, the mean connectivity of the silicate species decreases when the ratio SiO₂/Na₂O decreases.^{9,18}

Received: February 20, 2020

Revised: March 16, 2020

Published: March 25, 2020



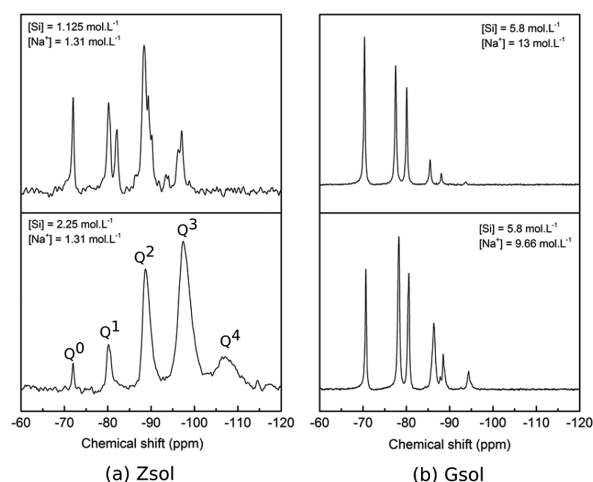


Figure 1. NMR spectra as a function of the chemical composition for (a) Zsol and (b) Gsol.

II.B. Simulated Solutions. In order to study the decondensation of Gsol and Zsol upon the addition of sodium hydroxide, we have first built two structures for the simulation. The stoichiometry and the connectivity of the initial structure have been chosen to be in agreement with the experimental data obtained for Zsol (see Table 1).

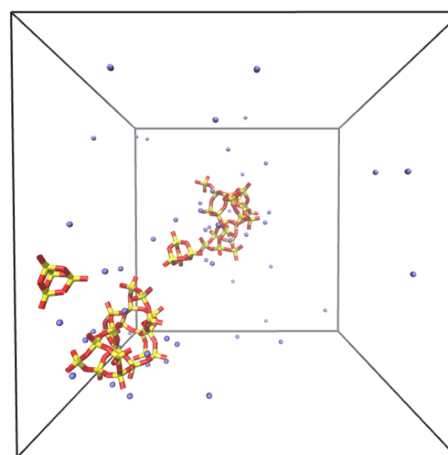
The two structures that has been simulated are given in Figure 2. The colloidal liquid is composed of 50 SiO_4 groups, initially organized in 4 silicate species, 2344 water molecules, and 28 Na^+ and OH^- groups. The simulation cell size has been set to $42 \times 42 \times 42 \text{ \AA}^3$ in order to correspond to the experimental density of 1.135 kg/m^3 . The system Gsol is composed of 40 SiO_4 groups, initially organized in 14 silicate species ranging from monomers to quadrimers, 294 water molecules, and 94 Na^+ and OH^- groups. The simulation cell size has been set to $30 \times 20 \times 20 \text{ \AA}^3$, in agreement with the experimental density that has been measured experimentally (about 1.35 kg/m^3).

II.C. Simulation Details. In order to simulate the effect of adding sodium hydroxide to these two systems, we have used a method based on the parallel tempering (PT) technique, which consists of replicating the initial state and running dynamics at different temperatures in order to enhance energy barrier crossing. After 10 steps, if it is energetically favorable, replicas are exchanged.^{19,20} As detailed by Dupuis et al.,¹⁶ in brief-PT, the simulation is interrupted regularly (herein every 1000 steps) and all replica are repopulated with the configuration that has been obtained at the lowest temperature. A set of 16 temperatures ranging from 300 to 800 K has been used.

In order to account for chemical reactions, we have used the reactive force field ReaxFF²¹ using the parameters given by Hahn et al.,²² in which parameters for Na are refitted on the basis of the parameters of Fogarty et al.²³ The parameters for Si/O/H have been previously tested and used to study various silicate systems.^{16,22,24,25} In particular, it is possible to reproduce the polymerization and depolymerization of silicates using this set of parameters. Moreover, for silica-base gel formation, this set of parameters has shown good efficiency to simulate the polymerization of pure silica gels.¹⁴

All simulations have been carried out with LAMMPS code using the python interface. The time step was set to 0.2 fs to ensure that the dynamics of water molecules is correctly

Zsol - precursor to zeolithe formation



Gsol - solution used to synthesize geopolymers

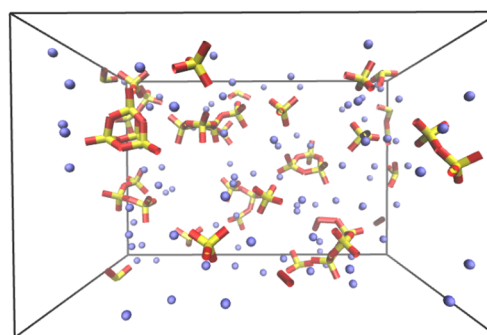


Figure 2. Snapshot of the original configurations. Silicon, oxygen, and sodium atoms are represented in yellow, red, and blue, respectively. The water molecules have been omitted for clarity.

described. The temperature has been controlled using the Nosé–Hoover thermostat.²⁶ Brief-PT runs were simulated using the NVT ensemble. If the average distribution of the Q^n does not evolve for 1000 steps, the convergence is achieved. For both systems, the convergence has been reached after about 200 ps of PT; note that this does not correspond to real time. The Q^n distributions have been compared to nuclear magnetic resonance measurements made after decondensation. The agreement with the experiments is good for both solutions (see Table 1). In the view of previous works, the brief-PT technique enables one to study decondensation in quantitative agreement with experimental data.^{16,17}

II.D. Statistical Analysis. In order to study the decondensation mechanism, we have proceeded to a statistical analysis along the trajectories that have been simulated. In particular, we have developed an algorithm to study the mechanism of decondensation (see Figure 3). In this algorithm, we are seeking for water molecules or hydroxides that enter the near environment during the dissociation, which defines one event. The environment of the dissociation, as shown in Figure 3, is the space defined by the sum of two spheres of radius R_c centered on the position of the two silicon atoms that are being dissociated. After each dissociation, we rewound the dynamics and counted the number of events that occurred during the last 250 000 steps of the simulation. Since water molecules can be dissociated in the near environment

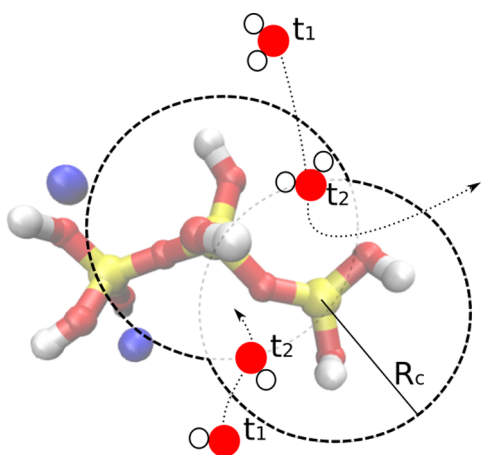


Figure 3. Graphical representation of the algorithm used to make the statistical analysis. In this algorithm, we consider two spheres of radius R_c centered on the two silicon atoms that are being dissociated. Each water molecule or OH^- that enters these spheres during the last 5 ps is counted (25 000 steps). Note that in PT, the time is not real-time but accelerated.

during the 5 ps, we record the number of events and the character of the event (entering of a water molecule or entering of an OH^- group) at the moment the molecule enters the dissociation environment.

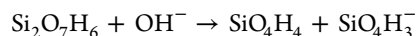
III. RESULTS AND DISCUSSION

III.A. Dissociation by Sodium Hydroxide. The first outcome of this work is that brief-PT increases the dynamics of dissociation and enables one to observe this complex process, which involves specifically many bond-breaking but also some bond-forming episodes. Validating if the simulation is reliable or not comes down to comparing the evolution of Q^n obtained by the simulation to the experimental data. In previous works,^{16,17} it has been shown that the polymerization and decondensation of silicates can be reproduced by this method. The decondensation can be due to either the breaking of a silicate chain or the opening of rings into a silicate chain.

In this work, we compare the decondensation on two different aluminosilicate solutions that are significantly different. The water to silicon ratio is equal to 47 in Zsol and 7 in Gsol. The sodium hydroxide concentration that will depolymerize the silicate chains is also modified accordingly with the experiments.

The decondensation of silicate chains in these systems has been previously reported.^{9,17} The values for the experimental and simulated systems are reported in Table 1.

III.B. Dissociation Mechanisms. The simplest dissociation mechanism for the silicate chains in the presence of OH^- groups is the following:



In our trajectories, we have observed more complex processes that are important to investigate in order to estimate the speed of the decondensation and if the dissociation of silicates will impact the pH of the solution by consuming OH^- groups or H_2O molecules (see Figure 4). In particular, we have found that the presence of additional water molecules or OH^- groups can reduce the energy barrier and favor bond-breaking.

In the mechanism shown in Figure 4, a water molecule first enters the dissociation environment. Quickly afterward, the water molecule is dissociated and the free proton protonates the silicate chain. Concurrently, the silicon is pentacoordinated by making a bond with the OH^- group. The pentacoordination is a necessary step for the decondensation,⁸ in a reversed process to the oligomerization.²⁷ Meanwhile, a second water molecule pulls away—in the opposite direction to the first water molecule—the oxygen atom of the Si–O–Si bridge (as shown in blue in Figure 4b). Finally, the Si–O–Si bond is dissociated. This example shows that these complex mechanisms involve not only a single hydroxide group to make the dissociation. This motivates a detailed study of the dissociation mechanisms.

III.C. Distance Probability Distribution. The distribution of Na–Si, Na–O, and Si–O distances gives insights on the dissociation mechanism. Figure 5 shows the distribution of oxygen atoms in the near environment to the silicon atoms that are being dissociated during 25 000 steps before dissociation. The first peak, located at 1.6 Å, corresponds to the bond distance of the Si–O covalent bond. For this peak, we observe that Zsol has a slightly shorter Si–O distance distribution than Gsol. This seemingly comes from the higher concentration of Na^+ in Gsol compared to Zsol, because cations may play a role in the strength of the Si–O bonds.²⁸ Herein, we observe that, in Gsol, the Si–O bond is longer and weaker than in Zsol. The small bump at about 2 Å seemingly comes from the Si–O bond distance during the dissociation that is being elongated.

Figure 6 shows the probability of finding an oxygen atom at a given distance from the sodium atoms during the 250 000 steps before dissociation. Note that only the oxygen from silicates has been considered to calculate the O–Na bond distance. Therefore, the very first peak, located around 1.6–2.0 Å, corresponds to the Na–O distance when Na^+ is in charge compensation and not the distance of the solvated ion with its first solvation layer. If we consider a Gaussian distribution, this peak is larger for Gsol ($\sigma = 0.84$ Å) than for Zsol ($\sigma = 0.76$ Å). For these curves, we observe that the sodium ions are localized both in the first (first peak) and in the second solvation layer (second peak) around the silicates during the decondensation.

The position of the second peak, around 2.4 Å, is consistent with the one calculated for sodium hydroxide solutions.²⁹ Nonetheless, in our calculations, we observe that at higher sodium hydroxide concentration, in Gsol, the peak is shifted to

Table 1. Table of Q^n for the Two Silicate Solutions^a

	Q_{exp}^0	Q_s^0	Q_{exp}^1	Q_s^1	Q_{exp}^2	Q_s^2	Q_{exp}^3	Q_s^3	Q_{exp}^4	Q_s^4
Zsol _i	1.5	0	4.8	4	21	24	53.6	52	19	20
Gsol _i	17.4	17	31	32	40	39	12	12	0	0
Zsol _f	11.2	12	16.5	16	52.7	45	19.5	22	0	5
Gsol _f	35.3	53.6	31.3	31.7	30.0	7.3	3.4	7.3	0	0

^aSubscripts: “exp” denotes the experimental value, “s” denotes the simulated value averaged over the last 5 ps of the simulation (see the Supporting Information), “i” denotes initial, and “f” denotes final.

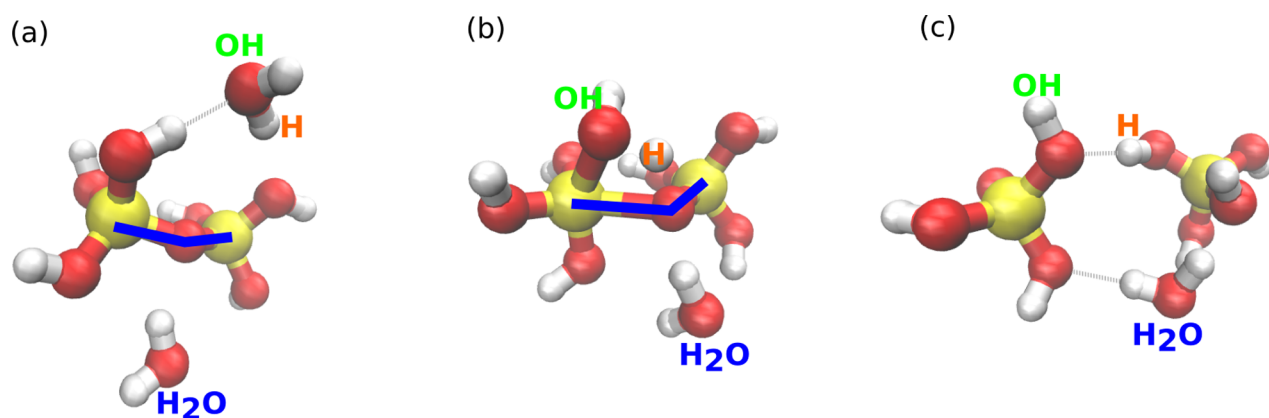


Figure 4. Example of a complex mechanism of dissociation. (a) In the first snapshot, a water molecule enters the dissociation sphere. (b) In second snapshot, this water molecule is dissociated, the hydrogen atom protonates a nearby silicate chain, and the OH^- group connects to a silicon atom. Meanwhile, a water molecule is pulling away the Si–O–Si bridge (as shown in blue in panel b). (c) In the last snapshot, the two silicates have been dissociated.

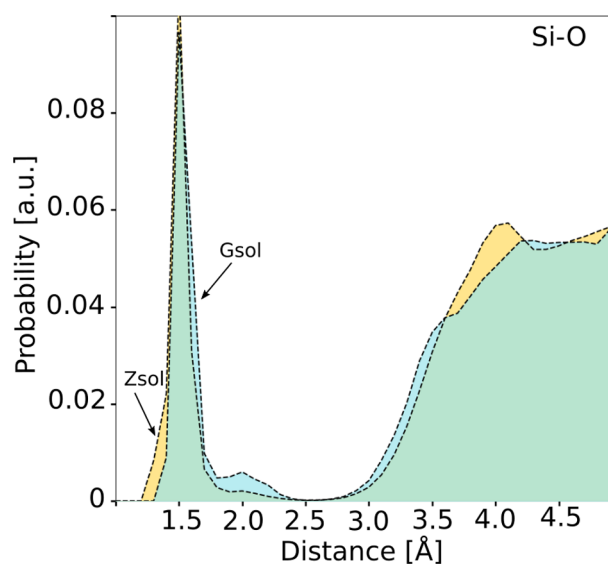


Figure 5. Probability of having an O atom at a given distance from a Si atom during the dissociation.

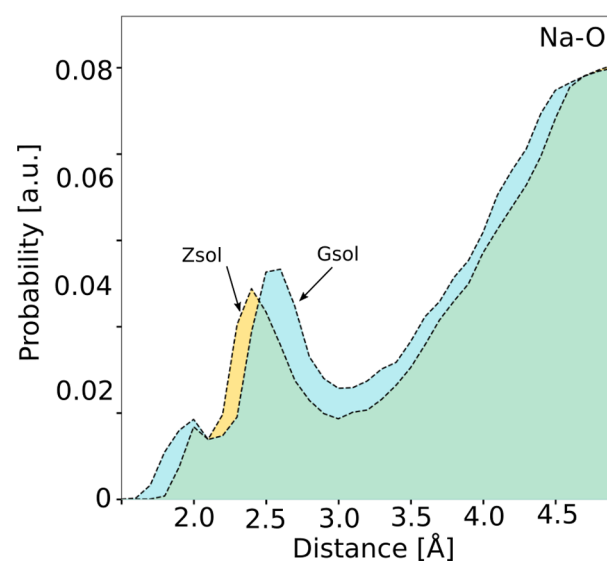


Figure 6. Probability of having an O atom at a given distance from a Na^+ cation during the dissociation.

slightly longer distances. In our calculations, we consider not only O_H but all the O atoms around Na^+ . Therefore, the shift of this peak could stem from the other O atoms in water molecules or silicates. The shift indicates that, at higher NaOH concentration and lower water/Si ratio, the second solvation layer is farther from the silicate groups.

Regarding the Si–Na distance probability distribution, shown in Figure 7, we observe a large first peak with a maximum at 3.2 Å for Gsol and 3.4 Å for Zsol. A reason for the Si–Na distance being reduced during the dissociation of alkali silicates in Gsol compared to Zsol could be that the $(\text{Na} + \text{Si})/(\text{H}_2\text{O})$ concentration is higher in Gsol. This also indicates that more Na^+ are in a charge compensation scheme in Gsol compared to Zsol.

III.D. Dilution by Pure Water. To compare, we have simulated the dissolution of both systems by a solution of pure water (with no sodium hydroxide), and we have found that, in the time-scale of the simulation, the silicate chains are not affected by dilution (i.e., Q^n does not evolve). This was thought to be due to the formation of rings that are self-protected structures in gels,^{14,16} but in Gsol, there is a low

quantity of rings and we observe that same effect. Therefore, in this mechanism, the passivation effect most probably comes from the presence of Na^+ . Na^+ is generally considered to elongate and weaken bonds (as observed in Figure 6). Therefore, the passivation effect could come from the protonation of the silicate chains that releases sodium ions in the solution. In these systems, Na^+ could protect the silicate chains if they are solvated by attracting molecules from their first solvation shell, in particular, water molecules and possibly OH^- . Hereinafter, we investigate the mechanisms of dissociation in more detail.

III.E. Angular Distribution Function. The O–Si–O angular distribution function, shown in Figure 8, is also an important piece of information when investigating how OH^- groups are added to the end of the chain or Si–O–Si bridges. A regular silica monomer has a single symmetric peak at about 109.5° that corresponds to the angle for an ideal tetrahedron. In the simulated phases, we observe a major peak located at 107° for Zsol and shifted to 105° for Gsol. Fitting the peaks with a Gaussian distribution gives a σ of 24° for Zsol and 27° for Gsol. The peak for Gsol is larger than for Zsol, which

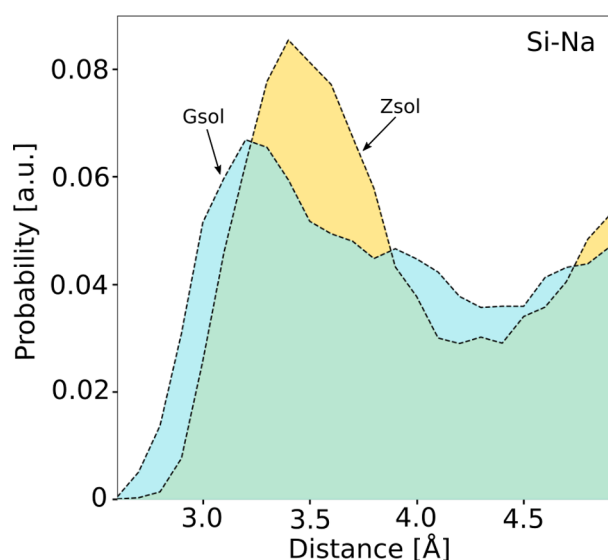


Figure 7. Probability of having a Na^+ cation at a given distance from a Si atom during the dissociation.

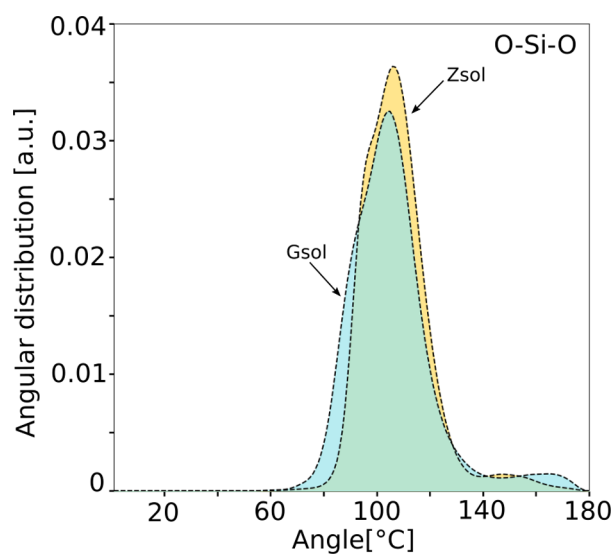


Figure 8. Angular distribution function of the O–Si–O angle in the silicon tetrahedron during dissociation.

indicates that it might be easier to make an additional Si–OH bond. It has been shown that for other elements, such as Al,¹³ the energy barrier to form pentamers is dependent on the flexibility of the AlO_4 or SiO_4 group. In particular, we can observe in Figure 8 that about 2% of the O–Si–O angles are larger than 140° . This corresponds to the opening of the angle during the bond dissociation.

III.F. Combined Role of Water and Hydroxide. To analyze the role of water and hydroxide during the dissociation of alkali silicates, we have plotted the number of events per dissociation. Each event being a water molecule or a hydroxide entering the dissociation environment, as explained previously and shown in Figure 3. In Figure 9, we have plotted the distribution versus R_{cut} . At small cutoff, for both systems, about 90% of the dissociations happens with a single event, whereas about 10% happens with the combined effect of two molecules (H_2O or hydroxides). There is an increase in the number of events for R_{cut} greater than 3.2 \AA . If we consider R_{cut} greater

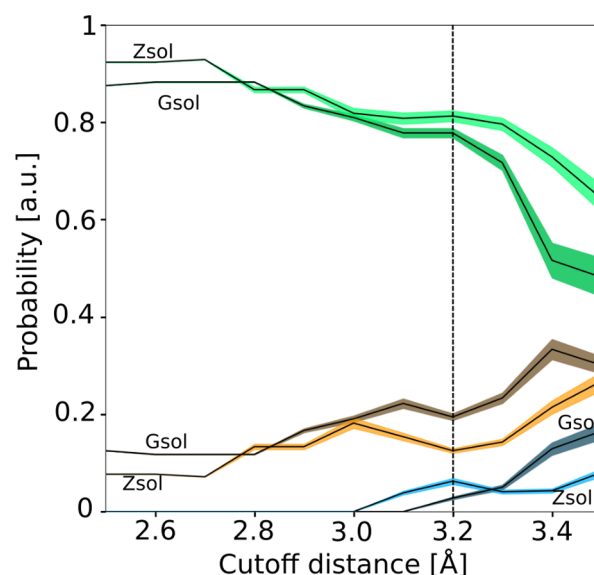


Figure 9. Probability of finding one (in green), two (in orange), or three (in blue) water molecules in the dissociation sphere versus the cutoff radius.

than 3.2 \AA , the number of dissociations with only one event suddenly drops to 60%, whereas it increases for two events and three events (25% with two events and 15% with three events). However, these additional molecules probably have a weak contribution to the dissociation.

In order to investigate the effect of having a secondary water molecule in the near environment, as observed in Figures 4 and 9, we have calculated the energy barrier for the dissociation (Figure 10). The energy barrier is about $50 \text{ kJ}\cdot\text{mol}^{-1}$.¹³ We observe a catalyst effect of the additional water molecule. The energy barrier is reduced by about $8 \text{ kJ}\cdot\text{mol}^{-1}$ (black and red lines), which corresponds to about 12% of the total energy barrier. Indeed, the pentacoordination of the silicon atom, necessary for the dissociation, is eased by the presence of the second water molecule as it pulls away the Si–O–Si bridge. Moreover, we observe that the dissociation in the presence of OH^- instead of H_2O is more favorable. Similarly, the addition of a water molecule reduces the energy barrier of about $5 \text{ kJ}\cdot\text{mol}^{-1}$. This indicates that correctly describing the chemistry of the environment is essential for reproducing the dynamics of polymerization and decondensation for silicates.

A non-negligible number of dissociations are due to the combined effect of hydroxide groups and water molecules. Although the dissociation is triggered by the addition of NaOH in our experiments, it has been shown that in other conditions, gels that contain alkali, such as alkali silica reaction gels, have higher connectivity than pure silica gels.^{16,30,31} In these gels, water is solvating ions, which allows for the formation of longer and more connected silicate chains. Further works should focus on trying to connect the solvation degree of ions to the connectivity of silicate chains in colloidal solutions and gels. Note that, for glasses, Na^+ is generally considered as a glass modifier, as it introduces defects due to a change in the local charge compensation scheme.³²

Understanding the decondensation mechanism is an important step toward the understanding of recondensation that occurs when adding aluminum to alkali-rich silicate solutions.⁹ Indeed, the reactivity and diffusion of aluminates with silicates should be related to how accessible reaction sites

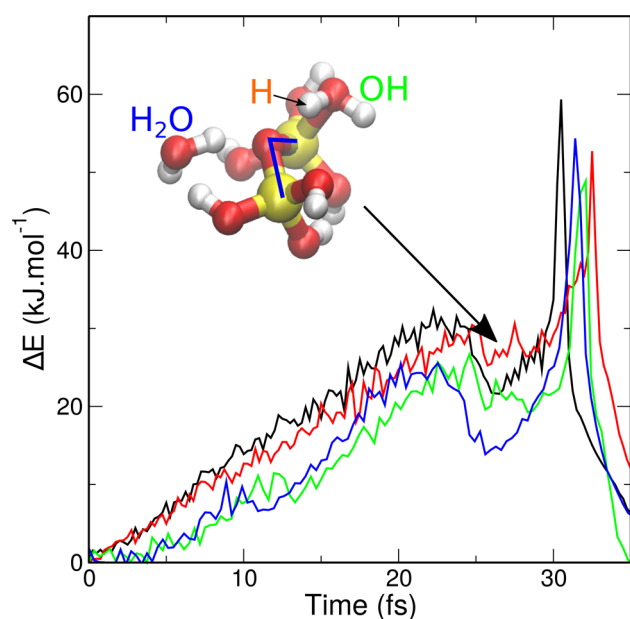


Figure 10. Energy barrier associated with the dissociation of an isolated silicate dimer with one water molecule (in black), two water molecules (in red), one OH^- group (in blue), or one OH^- and one water molecule (in green). Energy barriers have been obtained by molecular dynamics performed on a silicate dimer model. The snapshot corresponds to an intermediate state for the system with two water molecules just before the bond-breaking, in the same configuration as the one shown for the liquid in Figure 4b.

are and how the silicate structure can be penetrated. Decondensation is the first step toward the formation of aluminosilicate materials, such as geopolymers and zeolites. With sodium hydroxide solutions, silicates might be dissociated prior to reconcondensation.

This work could also have other implications, for instance, to elucidate the complex chemistry behind the formation of alkali silica gels during the so-called alkali–silica reaction known to cause irreversible damages in cement.^{33,34} This gel, which forms in water, is described in the literature from the experimental point of view, but little is known about the silicate structure. As we have shown in this work, water participates in the dissolution of silicate structures. Moreover, sodium ions interact with the silicate chains in a charge compensation scheme. The method presented herein could be used to study other solutions, such as sodium-rich solutions, in order to investigate the effect of alkali concentration.

IV. CONCLUSION

In conclusion, two solutions have been studied. Each system has a different silicon/water ratio and sodium/silicon ratio, but similar decondensation (due to the addition of sodium hydroxide) has been observed experimentally and by simulations. The brief-PT technique has been used to reproduce the decondensation of silicates, and the initial and final structures are in good agreement with the NMR experiments.

We have observed that dilution by pure water does not affect the connectivity of the silica chains. This indicates a passivation effect that is not only due to the presence of rings, as suggested in the literature, but most probably of Na^+ . In both systems, the dissociation of the silicates occurs in processes that involve mostly a single water molecule (or OH^-

group), but we have found that about 20% of the dissociations occurs with two water molecules (or OH^- group) in the first shell around the silicate chain. The water molecule reduces by about $8 \text{ kJ}\cdot\text{mol}^{-1}$ the energy barrier to dissociate the Si–O–Si bridge. The dissociation is also favored in the presence of OH^- groups. This could help to understand how to control the dissociation of silicates and the formation of alkali silicate or aluminosilicates, such as zeolites and geopolymers.

■ ASSOCIATED CONTENT

Supporting Information

The Supporting Information is available free of charge at <https://pubs.acs.org/doi/10.1021/acs.jpcc.0c01495>.

A figure showing the evolution of the connectivity Q during the simulation (PDF)

■ AUTHOR INFORMATION

Corresponding Author

Roland Dupuis – MIT/CNRS/Aix-Marseille Université Joint Laboratory "MultiScale Materials Science for Energy and Environment", UMI MSE2, Massachusetts Institute of Technology, Cambridge, Massachusetts 02139, United States; orcid.org/0000-0001-9451-1132; Email: rdupuis@mit.edu

Authors

Roland Pellenq – MIT/CNRS/Aix-Marseille Université Joint Laboratory "MultiScale Materials Science for Energy and Environment", UMI MSE2, Massachusetts Institute of Technology, Cambridge, Massachusetts 02139, United States; orcid.org/0000-0001-5559-4190

Jean-Baptiste Champenois – CEA, DES, ISEC, DE2D, SEAD, LCBC, F-30207 Bagnols-sur-Cèze, France

Arnaud Poulesquen – MIT/CNRS/Aix-Marseille Université Joint Laboratory "MultiScale Materials Science for Energy and Environment", UMI MSE2, Massachusetts Institute of Technology, Cambridge, Massachusetts 02139, United States; CEA, DES, ISEC, DE2D, SEAD, LCBC, F-30207 Bagnols-sur-Cèze, France

Complete contact information is available at:

<https://pubs.acs.org/doi/10.1021/acs.jpcc.0c01495>

Notes

The authors declare no competing financial interest.

■ ACKNOWLEDGMENTS

The authors acknowledge the The French National Research Agency (ANR) for financial support of the DYNAMISTE project (ANR-15-CE07-0013-02). This work was performed using HPC resources from GENCI- [TGCC/CINES/IDRIS] (Grant 2020-A0070911009). We would like to thank Donatien Gomes Rodrigues for NMR measurements.

■ REFERENCES

- Iler, R. K. *The Chemistry of Silica: Solubility, Polymerization, Colloid and Surface Properties and Biochemistry of Silica*; Wiley, 1979.
- Soules, T. F.; Gilmer, G. H.; Matthews, M. J.; Stolken, J. S.; Feit, M. D. Silica molecular dynamic force fields—A practical assessment. *J. Non-Cryst. Solids* **2011**, 357, 1564.
- Rejmak, P.; Dolado, J. S.; Stott, M. J.; Ayuela, A. 29Si NMR in Cement: A Theoretical Study on Calcium Silicate Hydrates. *J. Phys. Chem. C* **2012**, 116, 9755.

- (4) Li, F.; Josephson, D. P.; Stein, A. Colloidal assembly: The road from particles to colloidal molecules and crystals. *Angew. Chem., Int. Ed.* **2011**, *50*, 360.
- (5) Dupuis, R.; Benoit, M.; Nardin, E.; Méheut, M. Fractionation of silicon isotopes in liquids: The importance of configurational disorder. *Chem. Geol.* **2015**, *396*, 239.
- (6) Zhang, T.; Ge, J.; Hu, Y.; Zhang, Q.; Aloni, S.; Yin, Y. Formation of hollow silica colloids through a spontaneous dissolution–regrowth process. *Angew. Chem., Int. Ed.* **2008**, *47*, 5806.
- (7) Rimsza, J. M.; Du, J. Nanoporous silica gel structures and evolution from reactive force field-based molecular dynamics simulations. *npj Mater. Degrad.* **2018**, *2*, 18.
- (8) Dupuis, R.; Dolado, J. S.; Surga, J.; Ayuela, A. Tracing Polymerization in Calcium Silicate Hydrates Using Si Iso-topic Fractionation. *J. Phys. Chem. C* **2018**, *122*, 8356.
- (9) Aupoil, J.; Champenois, J.-B.; d’Espinose de Lacaillerie, J.-B.; Poulesquen, A. Interplay between silicate and hydroxide ions during geopolymerization. *Cem. Concr. Res.* **2019**, *115*, 426.
- (10) Manzano, H.; Moeini, S.; Marinelli, F.; van Duin, A. C. T.; Ulm, F.-J.; Pellenq, R. J.-M. Confined Water Dissociation in Microporous Defective Silicates: Mechanism, Dipole Distribution, and Impact on Substrate Properties. *J. Am. Chem. Soc.* **2012**, *134*, 2208.
- (11) Sulpizi, M.; Gageot, M.-P.; Sprik, M. The silica–water interface: How the silanols determine the surface acidity and modulate the water properties. *J. Chem. Theory Comput.* **2012**, *8*, 1037 pMID: 26593364.
- (12) Smith, M. E.; Holland, D. Atomic-Scale Structure of Gel Materials by Solid-State NMR. In *Handbook of Sol–Gel Science and Technology*; Klein, L., Aparicio, M., Jitianu, A., Eds.; Springer International Publishing: Cham, Switzerland, 2016; pp 1–43.
- (13) Dupuis, R.; Dolado, J. S.; Surga, J.; Ayuela, A. Doping as a Way To Protect Silicate Chains in Calcium Silicate Hydrates. *ACS Sustainable Chem. Eng.* **2018**, *6*, 15015.
- (14) Du, T.; Li, H.; Zhou, Q.; Wang, Z.; Sant, G.; Ryan, J. V.; Bauchy, M. Atomistic origin of the passivation effect in hydrated silicate glasses. *npj Mater. Degrad.* **2019**, *3*, 6.
- (15) Trinh, T. T.; Rozanska, X.; Delbecq, F.; Sautet, P. The initial step of silicate versus aluminosilicate formation in zeolite synthesis: a reaction mechanism in water with a tetrapropylammonium template. *Phys. Chem. Chem. Phys.* **2012**, *14*, 3369.
- (16) Dupuis, R.; Béland, L. K.; Pellenq, R. J.-M. Molecular simulation of silica gels: Formation, dilution, and drying. *Phys. Rev. Materials* **2019**, *3*, 075603.
- (17) Dupuis, R.; Gomes Rodrigues, D.; Champenois, J.-B.; Pellenq, R.; Poulesquen, A. Time resolved alkali silicate decondensation by sodium hydroxide solution. *J. Phys.: Mater.* **2020**, *3*, 014012.
- (18) Jansson, H.; Bernin, D.; Ramser, K. Silicate species of water glass and insights for alkali-activated green cement. *AIP Adv.* **2015**, *5*, 067167.
- (19) Swendsen, R. H.; Wang, J.-S. Replica Monte Carlo Simulation of Spin-Glasses. *Phys. Rev. Lett.* **1986**, *57*, 2607.
- (20) Jing, Z.; Xin, L.; Sun, H. Replica exchange reactive molecular dynamics simulations of initial reactions in zeolite synthesis. *Phys. Chem. Chem. Phys.* **2015**, *17*, 25421.
- (21) van Duin, A. C. T.; Dasgupta, S.; Lorant, F.; Goddard, W. A. ReaxFF: A Reactive Force Field for Hydrocarbons. *J. Phys. Chem. A* **2001**, *105*, 9396.
- (22) Hahn, S. H.; Rimsza, J.; Criscenti, L.; Sun, W.; Deng, L.; Du, J.; Liang, T.; Sinnott, S. B.; van Duin, A. C. T. Development of a ReaxFF Reactive Force Field for NaSiO_x/Water Systems and Its Application to Sodium and Proton Self-Diffusion. *J. Phys. Chem. C* **2018**, *122*, 19613.
- (23) Fogarty, J. C.; Aktulga, H. M.; Grama, A. Y.; van Duin, A. C. T.; Pandit, S. A. A reactive molecular dynamics simulation of the silica–water interface. *J. Chem. Phys.* **2010**, *132*, 174704.
- (24) Rimsza, J. M.; Du, J. Interfacial Structure and Evolution of the Water–Silica Gel System by Reactive Force-Field-Based Molecular Dynamics Simulations. *J. Phys. Chem. C* **2017**, *121*, 11534.
- (25) Du, T.; Li, H.; Sant, G.; Bauchy, M. New insights into the sol–gel condensation of silica by reactive molecular dynamics simulations. *J. Chem. Phys.* **2018**, *148*, 234504.
- (26) Martyna, G.; Klein, M.; Tuckerman, M. Nosé–Hoover chains: The canonical ensemble via continuous dynamics. *J. Chem. Phys.* **1992**, *97*, 2635.
- (27) Zhang, X.-Q.; Trinh, T. T.; van Santen, R. A.; Jansen, A. P. J. Mechanism of the initial stage of silicate oligomerization. *J. Am. Chem. Soc.* **2011**, *133*, 6613.
- (28) Méheut, M.; Schauble, E. A. Silicon isotope fractionation in silicate minerals: Insights from first-principles models of phyllosilicates, albite and pyrope. *Geochim. Cosmochim. Acta* **2014**, *134*, 137.
- (29) Coste, A.; Poulesquen, A.; Diat, O.; Dufrière, J.-F.; Duval, M. Investigation of the structure of concentrated NaOH aqueous solutions by combining molecular dynamics and wide-angle x-ray scattering. *J. Phys. Chem. B* **2019**, *123*, 5121 pMID: 31141363.
- (30) Vega, A. J.; Scherer, G. W. Study of structural evolution of silica gel using ¹H and ²⁹Si NMR. *J. Non-Cryst. Solids* **1989**, *111*, 153.
- (31) Hou, X.; Kirkpatrick, R. J.; Struble, L. J.; Monteiro, P. J. M. Structural Investigations of Alkali Silicate Gels. *J. Am. Ceram. Soc.* **2005**, *88*, 943.
- (32) Hehlen, B.; Neuville, D. R. Raman Response of Network Modifier Cations in Alumino-Silicate Glasses. *J. Phys. Chem. B* **2015**, *119*, 4093.
- (33) Kirkpatrick, R. J.; Kalinichev, A. G.; Hou, X.; Struble, L. Experimental and molecular dynamics modeling studies of interlayer swelling: water incorporation in kanemite and ASR gel. *Mater. Struct.* **2005**, *38*, 449.
- (34) Benmore, C.; Monteiro, P. J. The structure of alkali silicate gel by total scattering methods. *Cem. Concr. Res.* **2010**, *40*, 892.